ELSEVIER

Polymer 41 (2000) 6151–6160

polymer

Lattice modelling of penetrant diffusion through heterogeneous polymers

P.M. Hadgett, G. Goldbeck-Wood, A.H. Windle*

Department of Materials Science and Metallurgy, University of Cambridge, Pembroke Street, Cambridge, CB2 3QZ, UK

Received 26 May 1999; received in revised form 30 October 1999; accepted 11 November 1999

Abstract

We report on the development of a three-dimensional (3D) mesoscale lattice model of the diffusion of small gaseous penetrants in heterogeneous polymers. The model has been applied to the problem of predicting diffusional impedances caused by crystalline regions in semi-crystalline polymers. Increasing crystalline volume fraction and increasing crystal anisotropy both serve to reduce the diffusion dramatically. Although the trends observed with two- and three-dimensional lattices are similar, absolute values of impedances are much smaller in the case of the 3D lattice. The importance of using a 3D lattice when attempting quantitative prediction is therefore demonstrated. Validation of the 3D model is presented in the form of a comparison between experimental and model predictions of impedance in polyethylene. Crystals of different size, shape and crystalline volume fractions are used in the validation of the model.

Keywords: Diffusion; Lattice; Simulation

1. Introduction

Diffusion of small molecules through polymer membranes is a process that has important consequences in many technological industries, for example in the production of packaging materials [1] and separation membranes [2]. Throughout the last decade, simulation of this process has been carried out, mainly through the use of molecular dynamics on simplified models of bulk amorphous polymers. The aim of these studies has been to investigate the diffusion mechanism [3–6] and the effects of temperature [7–9], linking diffusion to various calculations of free volume [4,8,10–14] and more recently to predict quantitative values [15,16].

Possibly due to the size- and time-scale restrictions that are imposed by molecular dynamics few simulations have been carried out on less idealistic polymers, for example polymers with a significant amount of crystallinity, filled polymers or polymer blends. A notable exception is due to Müller-Plathe [17] who used a two-dimensional (2D) lattice model to study the effects of crystalline volume fraction and crystal shape on diffusion.

More than 50 years ago several analytical expressions for diffusion in heterogeneous media were developed on the basis of simple two-phase models [18]. These calculate diffusion coefficients from a knowledge of the volume fractions of the two phases and the diffusivities in each phase. Their disadvantages stem from the simplifications one has to make to derive such analytical equations. Common simplifications include the necessity of the dispersed phase to be regular shapes and that all components of the dispersed phase must be the same shape and size. Other analytical equations are only valid at very low dispersed phase concentration. These simplifications are serious drawbacks when attempting to predict quantitative values for diffusion in realistic systems. Semi-crystalline polymers, for example, rarely exhibit such uniformity in shape and size of crystal.

The lattice model of penetrant diffusion [17] (which we shall refer to simply as *the* 'lattice model') removes the need for many of these over-simplifications. It can account for different shapes of phases, different sizes of phases and can work at any volume fraction. It is also readily extended to the case of three or more phases, a feature that could be exploited to model interfacial regions between the distinct phases. Hence, this approach may provide a route to predicting diffusion through heterogeneous media in cases where the above simplifications are not valid, thereby bridging the gap between the analytical theories and molecular dynamics simulations.

In the current contribution we have studied the effect of semi-crystallinity on diffusion using a 2D lattice of a

* Corresponding author. Tel.: +44-1223-334321; fax: +44-1223-334567.

E-mail address: ahwl@cam.ac.uk (A.H. Windle).

0032-3861/00/$ - see front matter
PII: S0032-3861(99)00826-5

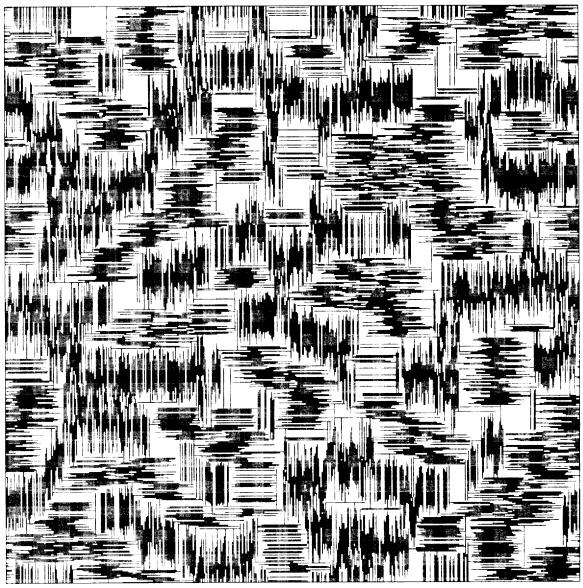

Fig. 1. Phase distribution on the lattice: 0.5 volume fraction, 1×35 shape.

mixture of permeable and completely impermeable regions. The model is used to investigate the retarding effect that crystals have on diffusion over a range of volume fractions and anisotropies. We have then extended the ideas presented by Müller-Plathe by developing the lattice model in three dimensions, and we present a comparison between the two types of lattice. Validation of the three dimensional model is presented in the form of comparison with two distinct sets of experimental data concerning diffusion in semi-crystalline polyethylene (PE).

2. Simulation details

In this section, we provide details of the development of the lattice algorithm to simulate diffusion through semi-crystalline polymers over appropriate distances.

2.1. Calculation of diffusivity

The diffusion coefficient of a penetrant may be calculated from a knowledge of the position of the penetrant over a period of time. In isotropic media, the diffusion coefficient can be calculated by the Einstein equation [19], i.e. assuming a random walk:

$$D = \frac{\langle |\mathbf{R}(t) - \mathbf{R}(0)|^2 \rangle}{2dt} \tag{1}$$

where $\mathbf{R}(0)$ and $\mathbf{R}(t)$ are the position vectors of the diffusing particle at times 0 and t, respectively, D is the diffusivity of the penetrant, d is the dimensionality of the system and the angled brackets denote averaging over the whole ensemble.

Practically, this means that the diffusion coefficient is readily obtainable from the gradient of penetrant mean-squared-displacement against time. Care must be taken to ensure that the length of the simulation is sufficient for Einstein diffusion to take place since, at short time-scales the mean-squared-displacement may not be linear with time, but linear to t^n with $n < 1$. This so-called anomalous diffusion is due to the motion of the penetrant being restricted in some way so as to make it non-random [20,21].

2.2. The lattice model

2.2.1. Development of code to predict the retarding effects of crystallinity

For the purposes of diffusion modelling, a semi-crystalline polymer is regarded as a heterogeneous system consisting of permeable amorphous regions and impermeable crystallites. The method for predicting the retarding effect of the microcrystals closely resembles that used by Müller-Plathe. Rather than constrain the simulations to two dimensions however, we have extended the model to three so that quantitative predictions become a realistic aim.

A Monte-Carlo algorithm produces a random walk on a cubic lattice under 3D periodic boundary conditions. The length of the lattice edge is 500 cells for the 2D work (giving 250 000 lattice sites) and 100 for investigations in three dimensions (giving one million lattice sites). The reduction in lattice-edge size in the 3D case is due to the restriction that computer memory places on the size of the lattice. Crystals are represented as impenetrable rectangles (2D) and rectangular parallelepipeds (3D) that are placed and orientated on the lattice to yield the desired crystalline volume fraction.

For placing the crystals on the lattice, our aim was not to mimic the mechanism of growth of crystals in any realistic manner, but rather to produce an end result that represented the final crystallinity well. Therefore, we employed a packing algorithm that simply places a crystal at a random position and random orientation on the lattice. If this move results in overlap with another crystal then the new crystal is deleted and a new attempt is made to place the crystal. This routine is then repeated until the correct crystalline volume fraction is reached. Figs. 1–4 show typical final (2D) lattices using this algorithm.

Fig. 1 shows the lattice with a crystalline volume fraction of 0.5 using crystals of dimensions 35×1. The short-range order between crystals arises due to the comparatively large aspect ratio of these crystals; if two crystals are parallel, with a spacing less than the long-edge of the crystal dimension, then it is not possible for a crystal to be placed between the two original crystals perpendicularly to those two. The only acceptable orientation is parallel to the crystals that are already placed. Thus, small regions of high orientation occur with crystals of large aspect ratio. Although this effect is not intentional on our part, it does go someway to represent the usual stacking effect that is observed in crystalline lamellae. Over large distances, however, there is no preferred orientation. This orientation over small distances will have some effect on the diffusion

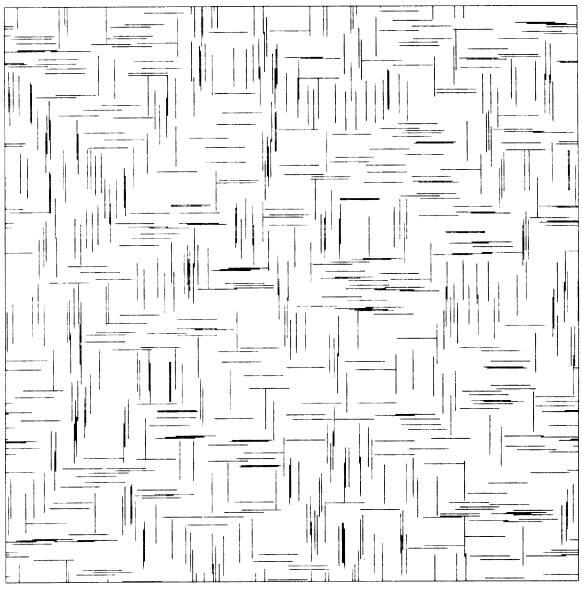

Fig. 2. Phase distribution on the lattice: 0.1 volume fraction, 1×35 shape.

of the penetrant in that area since diffusion is only possible parallel to the long axis of the crystal.

Fig. 2 shows a lattice with a much lower crystalline volume fraction (0.1) but with crystals of the same shape. Since there are fewer crystals, they are less constrained by their neighbours (which are further away) and so the short-range order is much less than at high volume fractions. Figs. 3 and 4 again show lattices at 0.5 and 0.1 crystalline volume fractions, but in this case the crystals are of dimension 1×5. This smaller aspect ratio means that the short-range order is much less, even at high crystalline volume fractions, because the crystals are less effective at imposing an orientation than crystals of larger aspect ratio. These types of effects are also present in three dimensions.

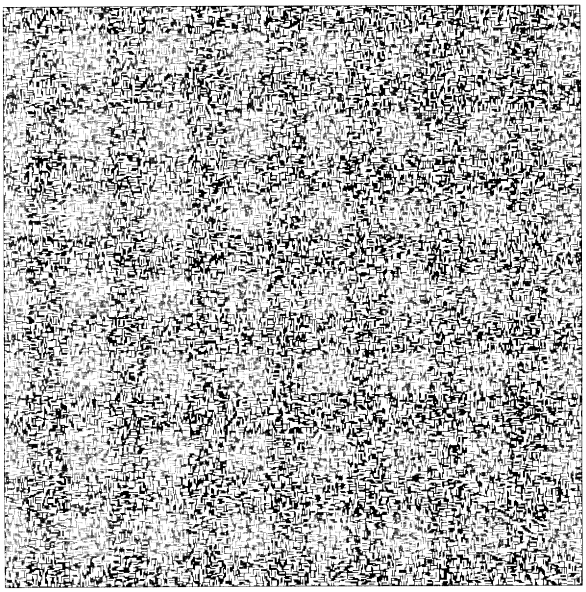

Fig. 3. Phase distribution on the lattice: 0.5 volume fraction, 1×5 shape.

At the beginning of each simulation, a starting point on the lattice is chosen at random. If the chosen position belongs to a crystalline region then a new random position is chosen until a crystalline-free region is found. In order to mimic the diffusional process, a direction in which to move is chosen at random (from a total of six in three dimensions and four in two dimensions). If the new position is free of crystalline material the random walker is moved to the new position. If the new position is blocked by a crystal, however, the move will not be carried out but the time-counter is still updated. The 'random walker' is moved in this manner for 10 000 000 time-steps for the generation of one set of positional data, which is then averaged over all time origins to give the mean-squared-displacement of the walker with time. Diffusion coefficients were calculated from the gradient of mean-squared-displacement against time (Eq. (1)). The final diffusion coefficient is based on an average of 5 separate runs on each of 5 different grids, thus averaging for position of crystallites on the grid and starting position of the random walker. Hence, each diffusion coefficient presented here is the average of 25 separate runs.

Using the above model, we have studied the effects of semi-crystallinity on diffusion in both two and three dimensions. Qualitative features we have looked at include the effects of crystalline volume fraction and the shape of the crystallites. In order to validate the model, work has been carried out that directly compares predictions made by the model and results found in the literature. The literature data discuss both qualitative and quantitative effects on diffusion of various crystalline shapes and distributions in PE.

3. Results and discussion

3.1. Qualitative effects of crystallinity

3.1.1. Two-dimensional lattice

The widely used measure of the effect of crystallinity on diffusion is 'impedance', i.e. the retarding effect of the crystallites, defined as the ratio of the diffusion coefficients of completely amorphous to semi-crystalline materials. Table 1 shows impedance data determined from our lattice model simulations. In the first instance, we considered square crystallites one lattice cell in size and a range of amorphous fractions.

As expected the impedance increases as more crystals are added to the lattice. It has been suggested [22] that the retarding nature of crystallites follows the empirical relationship

$$\frac{D_0}{D} = V_a^{-n} \tag{2}$$

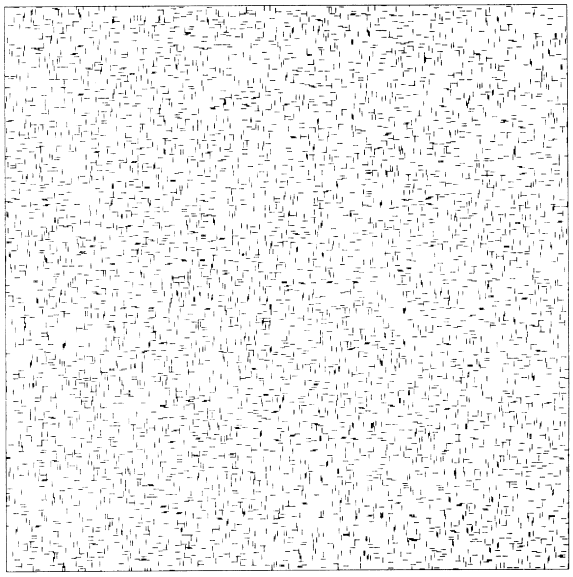

Fig. 4. Phase distribution on the lattice: 0.1 volume fraction, 1×5 shape.

where D_0/D is the impedance, V_a is the amorphous volume fraction and n is a constant exponent. We find that the data in Table 1 can be fitted by Eq. (2) with $n = 3.24$ (correlation coefficient of 0.97).

A similar investigation has been carried out for a variety of crystal shapes, keeping the single crystallite area to a constant size of 100 lattice sites. The results are shown in Table 2 and Fig. 5. The values for the power-law exponent n for the different aspect ratios of the crystals are given in Table 3.

As the aspect ratio increases so does the effective retarding power of the crystals. The trend of n with crystalline aspect ratio is well described by a logarithmic relationship of the form (correlation coefficient 0.97):

$$n = \ln(r) + 1 \tag{3}$$

where r is the crystal aspect ratio.

Thus for a given crystal size the following generalisations can be made. Firstly, as aspect ratio increases, the power of the crystal to stop diffusing molecules increases by virtue of the increased distance that the penetrant must travel to pass the crystal. Secondly, this rate of increase of n decreases as the aspect ratio increases as shown by the logarithmic trend.

Qualitatively these results agree well with those found by Müller-Plathe, since both sets of work highlight the increased retarding nature of crystals of higher anisotropy. Quantitatively the comparison is less straightforward, since Müller-Plathe's work dealt with different shapes and sizes.

Table 1
Impedance as a function of amorphous fraction for crystals of shape 1×1 on a 2D lattice

Amorphous fraction	1.00	0.95	0.90	0.85	0.80	0.75	0.70
D_0/D	1.00	0.95	1.24	1.39	1.82	2.25	3.01

Table 2
Impedance at a range of amorphous fraction and crystal shapes on a 2D lattice

Amorphous fraction	Crystal dimensions				
	100×1	50×2	25×4	20×5	10×10
1.00	1.000	1.000	1.000	1.000	1.000
0.95	4.365	1.663	1.151	1.250	0.997
0.90	5.921	2.196	1.371	1.348	1.120
0.85	6.913	3.279	1.559	1.627	1.251
0.80	10.96	4.489	1.798	1.822	1.280
0.75	10.88	5.722	2.209	2.100	1.425
0.70	12.24	6.254	2.745	2.367	1.652
0.60	39.35	10.31	4.073	2.592	1.859

Nevertheless, some comparison is still possible in the case of the square crystals and the effect of the side length. His work showed that the value of n increases as the size of crystal decreases, i.e. $n = 0.29$ (300×300), $n = 0.62$ (100×100) and $n = 0.94$ (20×20). Our values of $n = 1.32$ with a crystal size of 10×10, and $n = 3.24$ at 1×1 appear to be in agreement with this trend of increasing n with decreasing crystal size. Combing the above results lead to the following empirical equation for the effect of size of crystal on the power-law exponent n with a correlation coefficient of 0.98.

$$n = 3.3l^{-0.4} \tag{4}$$

where l is the length of the edge of the square crystal. Thus, in the case of square crystals, as the length of the side of the crystal increases the retarding power decreases for a fixed crystalline volume fraction.

3.1.2. Extension to three dimensions

Using our 3D version of the lattice model, we carried out a similar range of simulations as above. The effects of cubic crystals of size $1 \times 1 \times 1$ are shown in Table 4.

Again the retarding effect increases with crystalline fraction, but the effect is less pronounced than in the 2D case. The value of the exponent n is reduced to 2.20 (correlation coefficient 0.99) compared to 3.24 in the 2D case. This indicates merely that it is harder to stop a random walker in three dimensions where there are six possible directions for movement than in two dimensions where there are only four available directions. More importantly, it highlights the necessity of working in three dimensions if quantitative values, rather than mere trends, are to be predicted.

The effect of crystal shape in three dimensions was studied by considering a range of surface area to volume ratios, keeping the volume fixed at a size of 1000 lattice sites. This condition allowed a total of nine different shapes. The impedance data determined from our simulations are shown in Table 5 and Fig. 6.

As the ratio, r, of surface area to volume increases, i.e. as

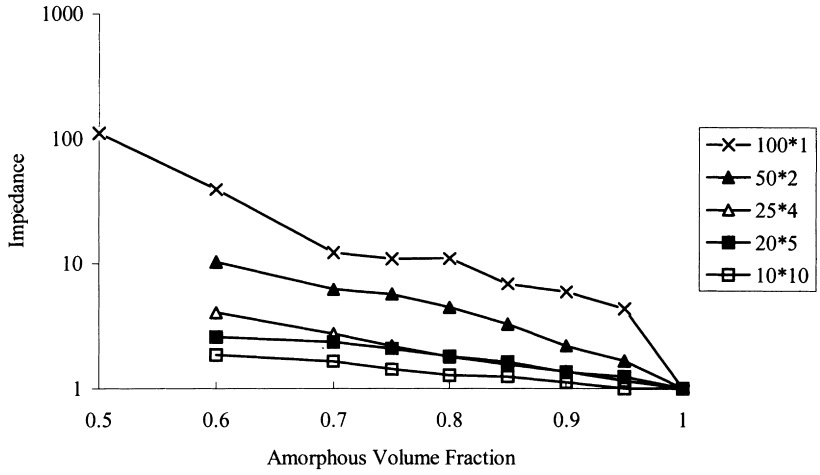

Fig. 5. Impedance at a range of amorphous fraction and crystal shapes on a 2D lattice.

the crystals become less isotropic, the retarding effect of the crystals increases. Again whilst the general trends are similar to the trends seen with the 2D work, the quantitative effects are much smaller here. In fact, a linear fit was found to be more accurate than a power law fit. Furthermore, analysis of our data suggests that we can factorise the effects of crystalline volume fraction and shape: the impedance increases linearly with volume fraction at constant shape, and is also linear in r at constant volume fraction. In order to satisfy the known boundary condition that as the amorphous content tends to zero impedance tends towards infinity we have included a $(V_a)^{-1}$ term. Hence, we get

$$\frac{D_0}{D} = 1 + \frac{ArV_c}{V_a} \tag{5}$$

where V_c is the crystalline volume fraction, i.e. $V_c = 1 - V_a$, r is the ratio of surface area to volume and A is a constant given a fixed volume of crystal. The best fit gives a value of $A = 1.02$ and a correlation coefficient between calculated and actual impedance data of 0.96. It would appear that the above equation is sufficient to describe the impedance effect accurately, at least in the range of crystalline volume fractions and crystal shapes studied here.

Finally we investigated the effect of a distribution of crystal shapes within one 'material'. We used the same shapes as above and kept the crystal volumes at 1000 lattice sites, but now chose an equal number of crystals of each shape. The resulting data, given in Table 6, have been fitted by a linear regression, yielding:

$$\frac{D_0}{D} = 1 + 1.466\frac{V_c}{V_a} \tag{6}$$

which has the same form as Eq. (5). We can hence equate

$$Ar = 1.466 \tag{7}$$

Since A is independent of crystal shape and volume fraction, we can substitute the value of $A = 1.02$ determined above and hence we find a value of $r = 1.44$. It appears that the effective surface area to volume ratio of a distribution of shapes lies somewhat above the mean value at $r = 1.16$. The conclusion is that the less isotropic shapes play a more dominant role than the more isotropic shapes at retarding diffusion.

Table 3
Correlation of n (as defined in Eq. (2)) with aspect ratio of crystal on a 2D lattice

Crystal dimension	Aspect ratio	n
100×1	100	5.45
50×2	25	4.41
25×4	6.25	2.76
20×5	4	1.89
10×10	1	1.32

3.2. Quantitative validation

Although the previous work is useful for highlighting general trends, it is of course the ultimate aim of modelling to be able to predict quantitative values found in experimental reality. Although the model described above has several limitations, it was still thought useful to attempt quantitative prediction. For a proper validation of our model, we require experimentally determined diffusivities for a small molecule through a semi-crystalline polymer and the diffusivity in a purely amorphous sample of the same polymer. A proper characterisation of the crystallinity in the polymer is also needed, in the form of crystalline volume fraction and shape and size of the crystals. Thus, the two following sections report studies in which the model is used to predict quantitative features of crystalline impedance effects that can be compared to experimental data found in the literature.

3.2.1. Quantitative validation 1

Michaels and Bixler [22] have investigated the diffusion

Table 4
Impedance as a function of amorphous fraction for crystals of shape $1 \times 1 \times 1$ on a 3D lattice

Amorphous fraction	1.00	0.95	0.90	0.85	0.80	0.75	0.70	0.65	0.60	0.55	0.50
D_0/D	1.00	1.08	1.13	1.28	1.45	1.56	1.94	2.27	2.59	3.11	5.17

of small gases through various samples of PE that contain varying crystalline fraction and crystal shape. They proposed that two impedance factors operate together to reduce the diffusion coefficients in semi-crystalline PE and proposed an expression:

$$D = \frac{D^*}{t\beta} \tag{8}$$

where D^* is the diffusion coefficient in a hypothetical completely amorphous PE and t is a geometric impedance factor accounting for the reduction in diffusion due to the necessity of penetrants having to diffuse around crystallites. β is a chain immobilisation factor which takes into account the reduction in amorphous chain segment mobility due to the proximity of the crystallites. Our model addresses t, the geometric impedance factor but does not account for β. Fortunately, Michaels and Bixler devised a technique to separate impedance into these two terms and so it is possible for us to validate our model against their data for t. For small penetrants we have assumed the effects of the reduction in chain segment mobility is likely to be small.

The crystallites in PE are thought to be lamellae and chain-folded [23]. The lamellae are 70–150 Å in thickness with the other dimensions possibly extending into the micron range. During cooling from the melt, stacks of crystalline lamellae interleaved with amorphous layers form. In addition, a secondary structure, the so-called spherulite, is formed as the lamellae grow radially outward from nucleation centres. Experimental evidence [24] suggests that the basic impenetrable unit within PE is the lamella and not the spherulite. The model at present ignores any effects that the spherulitic structure might have on the diffusion, though it is envisaged this could be included in the model in future as the seemingly inexorable increase in computing power allows lattices of larger size and higher resolution.

The types of crystallinity in PE that Michaels and Bixler used are shown in Table 7, where the crystals were of shape $a \times a \times b$ and the lamella crystal thickness $b = 1$. The crystalline volume fractions were measured using density measurements made in density gradient columns. The crystal aspect ratios were determined by fitting Fricke's equation (Eq. (9)) to diffusional impedance data for each of the polymers. Although it would be preferable to compare the lattice model with experimental data directly, in this case, we are actually comparing the lattice model to the predictions made by the Fricke analysis.

For this study the number of grids was increased to 10 and the number of diffusion runs on each grid was also increased to 10. The linear lattice dimension was increased to 150, giving 3 375 000 lattice sites. Despite this increase in size, it was not always possible to represent the crystal-amorphous microstructure at the correct proportion. For example, in the case of Hydropol where the ratio of lateral size to thickness is $a/b = 8$, the crystal representation was of size $1 \times 8 \times 8$. Thus one lattice length corresponds to approximately 100 Å, and the minimum spacing between crystallites is therefore also 100 Å. It would be preferable to scale the size of the crystals up to $4 \times 32 \times 32$ which would represent accurately not only the shape of the crystal but also its size in relation to the inter-crystal spacing which is approximately a quarter of the width of a crystal. On a lattice of size 100 this is just possible in the case of Hydropol, but it is not possible for the Alathan and Grex polymers, since scaling their crystals gives crystals of length 98 and 140. Clearly this is something that could be easily achieved with greater computing power, but it is hoped that

Table 5
Impedance at a range of amorphous volume fraction and anisotropies on a 3D lattice

	Crystal shape								
	$10 \times 10 \times 10$	$10 \times 20 \times 5$	$5 \times 8 \times 25$	$4 \times 10 \times 25$	$4 \times 5 \times 50$	$2 \times 20 \times 25$	$2 \times 10 \times 50$	$1 \times 40 \times 25$	$1 \times 20 \times 50$
	Surface area:volume								
V_a	0.6	0.7	0.73	0.78	0.94	1.18	1.24	2.13	2.14
1.00	1.00	1.00	1.00	1.00	1.00	1.00	1.00	1.00	1.00
0.95	1.02	1.07	1.02	1.04	1.03	1.09	1.10	1.29	1.22
0.90	1.06	1.06	1.09	1.10	1.09	1.18	1.20	1.43	1.48
0.85	1.11	1.16	1.12	1.18	1.13	1.25	1.31	1.67	1.70
0.80	1.15	1.19	1.19	1.20	1.18	1.36	1.46	1.78	1.80
0.75	1.18	1.27	1.24	1.27	1.28	1.52	1.53	1.94	1.90
0.70	1.29	1.32	1.32	1.39	1.43	1.53	1.63	2.12	2.04
0.65	1.32	1.36	1.39	1.46	1.45	1.66	1.74	2.14	2.24
0.60	1.44	1.46	1.44	1.48	1.58	1.77	1.83	2.33	2.26

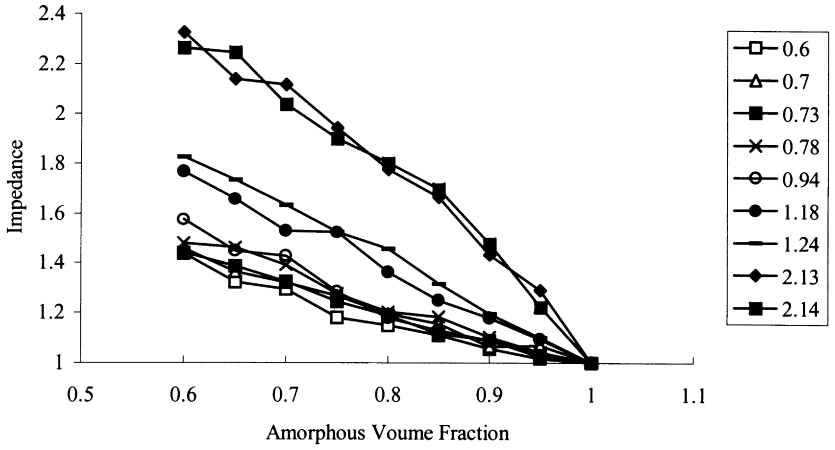

Fig. 6. Impedance at a range of amorphous volume fraction and anisotropies on a 3D lattice.

we may still arrive at reasonable values using just the shape of the crystals. In the cases of high crystalline content and high anisotropy, it was not always possible to pack the crystals onto the lattice using a random position and orientation. In these cases a trend was produced that encompassed the data where it was possible to fit the crystals on the lattice.

In order to fit our data to an analytical equation, we employ a much-used relationship originally suggested by Fricke [25]

$$I = \frac{x + (1 - V_a)}{xV_a} \tag{9}$$

where I is the diffusional impedance, x is an anisotropy parameter and V_a is the amorphous volume fraction.

This equation was derived originally for the prediction of electrical conductivity for disperse systems containing a spheroidal second phase. The parameter x is a function of the shape of the spheroids which is large for isotropic crystals and vice versa. It is used as a fitting parameter in subsequent work. Naturally, there is some concern regarding using such fits to extend the relationship beyond the boundaries of the data which was used to produce the fit. Indeed, it should soon be possible to design a sufficiently large lattice to allow any shape and size crystal distribution within the constraints of computer memory. For now, simple empirical extension of our data must suffice. It should be noted that the Fricke equation is very similar in form to the empirical relationship that was derived in an earlier section (Eq. (5)). The empirical equation uses a simpler measure of shape—namely the aspect ratio. However, the empirical equation is obtained from only a small amount of data (small volume fraction range and no account of changes in crystal size is accounted for) and is thus not ideal.

Table 6
Impedance as a function of amorphous fraction with a distribution of crystal shapes on a 3D lattice

V_a	1.00	0.96	0.91	0.87	0.82	0.78	0.73	0.69	0.62
D_0/D	1.00	1.07	1.19	1.29	1.41	1.52	1.62	1.68	1.82

Fig. 7 shows an example of a Fricke fit to the diffusional data from our model and also the extension of that fit to the realistic crystalline volume fraction. The data used in the example relate to the polymer Grex and the correlation coefficient between data and the Fricke fit is 0.99. Using the Fricke relationship, the predicted values for the impedance effect of the different types and volume fractions of crystals (shown in Table 8) are within 20% of the experimental values, though some values are much better than that.

In the case of Hydropol it was possible to model the microstructure at the correct ratio of crystal amorphous layers, as well as correct shape thus removing the need for fitting and extrapolation. A range of sizes was investigated starting from the size used in the original work above and increasing to the correct size. The data in Table 9 show that increasing the size of the crystal decreases the retarding effect to a figure that is in excellent agreement with the experimental value of 1.43. This indicates that in order to obtain quantitative values of impedance it is necessary to use the correct size of crystal as well as the correct shape. Using the current lattice it was impossible to model the crystals of the other polymers at the correct size and this is one way in which the model could be improved in the future.

3.2.2. Quantitative validation 2

A second set of experimental data for comparison with the model has been taken from the PhD thesis [26] of Dr Sally Harding from the Department of Chemical Engineering at Cambridge University. The data were obtained by means of the pulsed gradient spin echo (PGSE) NMR method [27]. This technique extends the range of diffusivities that can be measured to values that are significantly lower than can be detected by other methods. Harding measured the diffusivity of benzene in samples of PE with

Table 7
Amorphous volume fractions and crystal shape for three polyethylenes

Polymer	V_a	a/b
Grex	0.23	35
Alathon	0.57	23
Hydropol	0.71	8

Table 8
Experimental impedance values of the crystals in three polymers along with simulation results

	t (experimental)	t (fixed size)
Grex	6.4	7.09
Alathon	3.2	2.49
Hydropol	1.43	1.77

differing amounts of crystallinity. The crystallites were assumed to have an aspect ratio of $4 \times 100 \times 100$. This is in accordance with the results reported by Hedenqvist et al. [28] who, in a study of the morphology of a range of semi-crystalline PE samples, derived the lamellar thickness from differential scanning calorimetry measurements and the lateral extent of the lamellae from transmission electron microscopy. As in the previous example, it is assumed that the basic impenetrable unit within PE is the lamella and not the spherulite. The three samples of PE have amorphous volume fractions of 27, 49 and 67%. The diffusion coefficient of benzene in a purely amorphous sample of PE was not measured, so this value was taken from the average of literature values (4.5×10^{-11} m^2 s^{-1}). The above value is used, along with the experimental data of Harding, to calculate diffusional impedances, and these data are shown in Table 10.

We have used our three-dimensional implementation of the lattice diffusion model to estimate the impedance in the semi-crystalline samples described above. As in the previous case, it was difficult to use the correct size of crystal in three dimensions due to the size restrictions imposed by the lattice size. Nevertheless it was possible to use crystals of size $3 \times 75 \times 75$ and so this size was used for the simulations. For the cases of 68 and 49% amorphous volume fraction, it was possible to obtain direct values from the model. However, is was not possible to create a lattice of 27% amorphous volume and a Fricke fit was used to extend the trend to this case.

Impedance data from the lattice model at a range of crystalline volume fractions are shown in Table 11, alongside the impedance values from experiment and impedance values calculated using a 2D lattice for comparison. In the case of 27% amorphous volume fraction the Fricke fit gave a correlation coefficient of 0.99. The 2D lattice results in impedances that are too great, giving an average error of 70% compared to the impedance data that used a literature value for the diffusion in the pure amorphous polymer. This level of error is greatly improved upon by using the three-dimensional lattice, which gave errors of 3 and 9% for the cases of 27 and 49% amorphous volume fraction, respectively. In the case of an amorphous volume fraction of 68% the error is larger at 36%, though this is still more than twice as accurate as the value predicted by the two dimensional lattice. The literature value of diffusion in the purely amorphous polymer that was used in the calculation of experimental impedances is an average value. The predictions made in the cases of 27 and 49% amorphous volume fraction are well within the spread of impedances if different literature values are used. The prediction at 68% amorphous volume fraction remains somewhat too high.

Finally, we note that increasing the crystallite size from $1 \times 25 \times 25$ to $2 \times 50 \times 50$ and then to $3 \times 75 \times 75$ resulted in a small decrease in the impedance values predicted by the model. This finite size-effect was also observed in the first quantitative validation and in the case of square crystals by Müller-Plathe. The decrease in impedance values translates to an improvement in the agreement between the model and experimental data. It can hence be expected that a

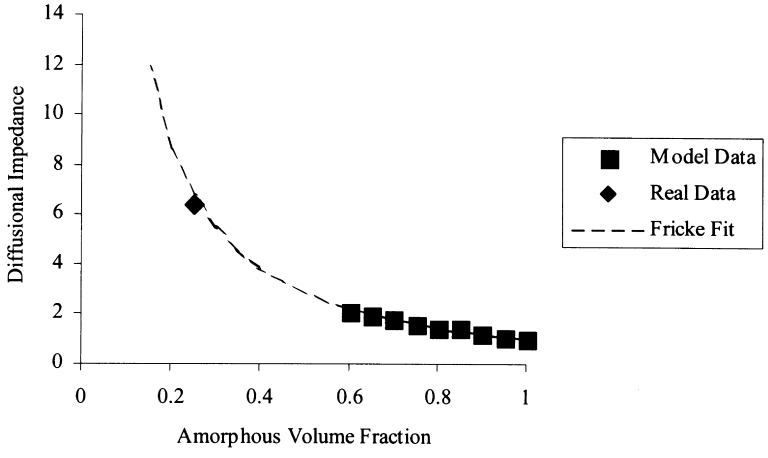

Fig. 7. Fricke fit to impedance data for the polymer Grex on a 3D lattice.

Table 9
Size effect on the impedance of crystals for Hydropol

Size of crystal	D_0/D
$1 \times 8 \times 8$	1.77
$2 \times 16 \times 16$	1.49
$3 \times 24 \times 24$	1.47
$4 \times 32 \times 32$ (correct size)	1.41

simulation run at the correct size of $4 \times 100 \times 100$ should result in further improvement.

4. Conclusions

We have extended a lattice model first used by Müller-Plathe to three dimensions. Using such a model, diffusion in semi-crystalline polymers has been investigated both qualitatively and quantitatively. In order to represent semi-crystalline media the second phase (the crystal) is modelled by an impenetrable object.

The retarding effects of crystals have been investigated in both two and three dimensions. We have shown that high content of crystallinity and high anisotropy of crystals both serve to increase the impedance. This effect is much less pronounced in three dimensions than in two since it is easier to prevent the motion of the random-walker when it only has four possible directions (in two dimensions) compared to when it has six possible directions in which to move (three dimensions). Predictions of quantitative values of impedance have been made for several cases of polyethylene. Using the correct shape of crystal (but not the correct size in relation to the mean inter-crystal spacing because of the restrictions of the lattice size), generally produces values that are within $\pm 20\%$ of the experimental value. In cases of high anisotropy, it was not possible to place the crystals at random at the correct volume fraction and the impedance had to be calculated from extrapolation from lower crystalline volume fractions. In these cases, a fit of the form suggested by Fricke appears to work well. In the case where it was possible to model the inter-crystal spacing accurately excellent agreement with experiment has been achieved. Using this simple model, the retarding effects of crystallinity on diffusion can be simulated rather well.

It would be possible to refine the 'semi-crystalline' model further. A larger lattice would allow accurate inter-crystal spacing even for the highly anisotropic crystals and would also allow crystals of even greater anisotropy to be used, thus circumventing the need for any extrapolation or empiricism. One method by which this could be achieved is to change the way in which the lattice is stored internally; rather than store the whole lattice explicitly, simply storing the corners of the crystals would dramatically reduce the amount of memory that is needed. Although the effects of spherulites have been assumed to be small, an increased resolution and size of lattice would be able to test this hypothesis.

The second obvious enhancement would be to alter the random manner in which crystals are placed on the lattice. A more realistic microstructure, in the form of stacks of crystalline and amorphous layers, and higher crystalline volume fractions, should be possible with an improved crystal-placing algorithm. It should also be possible to impose a distribution of crystal sizes that more accurately reflects that found in reality given sufficient experimental data. Finally, it may be possible to generate sufficient data to allow the calculation of an empirical equation encompassing size, shape and volume fraction simultaneously, therefore dispensing with the need to carry out explicit simulations at all.

Alongside the improvements to the model that are mentioned above, there are several possibilities for future work by extending the applicability of the model. Firstly, it may be possible to include a third region representing the interface between crystal and amorphous regions. If the diffusion characteristics of penetrants in this third region can be determined, perhaps through the use of molecular dynamics simulations, then it would be possible to have a more realistic model of the semi-crystalline polymer. Recent work has shown the diffusion in clay–polymer nanocomposites also to be a promising area of study for this model.

Table 10
Crystalline volume fractions and sizes for the three samples of PE with diffusional impedances calculated using literature data for the value of the diffusion coefficient in purely amorphous PE

Polymer	V_a	Literature impedance
1	0.27	5.29
2	0.49	2.64
3	0.68	1.36

Table 11
Diffusional impedances calculated using simulation and literature values for the diffusion coefficient in purely amorphous PE with predictions made using a 2D and a 3D lattice

Polymer	Model impedance		
	3D	2D	Literature impedance
1	5.45	9.09	5.29
2	2.90	4.11	2.64
3	1.86	2.44	1.36

Acknowledgements

The authors would like to thank Dr S. Harding for her generous permission to use the experimental data in Section 3.2.2 that she obtained as part of her PhD thesis at Cambridge University. We would also like to thank Professor H. Hopfenberg for useful discussions concerning this work. In addition, the authors would like to

thank Hoechst-Celanese for financial funding for this work.

References

[1] Ashley RJ. In: Comyn J, editor. Polymer permeability, London: Elsevier Applied Science, 1985.
[2] Fels M, Li NN. Permeability of plastic films and coating to gases, vapors and liquids. In: Hopfenberg HB, editor. Polymer science and technology, 6. New York: Plenum Press, 1974.
[3] Müller-Plathe F. Acta Polym 1994;45:259.
[4] Sok R. Permeation of small molecules across a polymer membrane: a computer simulation study, PhD Thesis, University Of Groningen, 1994.
[5] Gusev AA, Müller-Plathe F, VanGunsteren WF, Suter UW. Adv Polym Sci 1994;116:207.
[6] Müller-Plathe F. J Chem Phys 1992;96:3200.
[7] Han J, Boyd RH. Macromolecules 1994;27:5365.
[8] Han J, Boyd RH. Polymer 1996;37:1797.
[9] Pant PVK, Boyd RH. Macromolecules 1992;25:494.
[10] Gee RH, Boyd RH. Polymer 1995;36:1435.
[11] Takeuchi H, Okazaki K. Makromol Chem Macromol Symp 1993; 65:81.
[12] Takeuchi H, Roe RJ, Mark JE. J Chem Phys 1990;93:9042.
[13] Arizzi S, Mott PH, Suter UW. J Polym Sci Part B: Polym Phys 1992;30:415.
[14] Arizzi S, Suter, UW. Abstracts of Papers of the American Chemical Society, 19, 107-PMSE, 1989.
[15] Fukuda M, Kuwajima S. J Chem Phys 1997;107:2149.
[16] Hofman D, Ulbrich J, Fritsch D, Paul D. Polymer 1996;37:4773.
[17] Müller-Plathe F. Chem Phys Lett 1991;177:527.
[18] Crank J. The mathematics of diffusion. 2. Oxford, UK: Oxford University Press, 1956.
[19] Allen MP, Tildesley DJ. Computer simulation of liquids. Oxford, UK: Oxford University Press, 1987.
[20] Takeuchi H, Okazaki K. Mol Simul 1996;16:59.
[21] Müller-Plathe F, Rogers SC, van Gunsteren WF. Chem Phys Lett 1992;199:37.
[22] Michaels AS, Bixler HJ. J Polym Sci 1961;50:413.
[23] Keller A, Goldbeck-Wood G. In: Aggarwal SL, Russo S, editors. Comprehensive polymer science suppl., II. Oxford, UK: Pergamon Press, 1996.
[24] Michaels AS, Bixler HJ. J Polym Sci 1961;50:393.
[25] Fricke H. Phys Rev 1924;24:575.
[26] Harding S. NMR studies of structure transport relationships in porous media: liquid diffusion in polymers, PhD thesis, University of Cambridge, 1998.
[27] Stejskal EO, Tanner JE. J Chem Phys 1965;42:288.
[28] Hedenqvist M, Angelstok L, Larsson PT, Gedde UW. Polymer 1996;37:2887.